Air Quality, Atmosphere & Health (2025) 18:1087–1099
https://doi.org/10.1007/s11869-025-01702-x

Health for the future: spatiotemporal CA-MC modeling and spatial pattern prediction via dendrochronological approach for nickel and lead deposition

Oznur Isinkaralar[1] · Kaan Isinkaralar[2] · Hakan Sevik[2]

Received: 25 November 2024 / Accepted: 17 January 2025 / Published online: 28 January 2025
© The Author(s), under exclusive licence to Springer Nature B.V. 2025

Abstract
Nonpoint source pollution (P_{NS}) poses a significant environmental challenge owing to its adverse impacts on public health and ecological sustainability. Knowing the spatial pattern of heavy metals (HMs), one of the toxic substances, in the organization of urban space and the production of zoning decisions, both in the selection of pollution sources and living spaces, is immensely guiding today and in the future. The city of Düzce may be susceptible to public health risks attributed to the accumulation of HMs from escalating urbanization activities. This study aims to reach the reasons of P_{NS} by modeling nickel (Ni) and lead (Pb) concentrations, their spatial distributions, and how they may be spatially in the future. For Ni and Pb toxic substances, accumulation was analyzed based on annual tree rings (ATRs) of the same species, and future predictions were made based on the complex structure of the spatial pattern. The concentrations accumulated in *Picea orientalis* L. ATRs between 2018 and 2023 were analyzed. Predictions of 2028 were produced according to the low > middle > high classification by dividing the space into 500 × 500 m grids via Geographic Information Systems (GIS). The accuracy of the produced model was determined as $R^2 = 0.9412$ for Ni and $R^2 = 0.9882$ for Pb. Design strategies at different scales were presented with a novel approach by examining the plan decisions of the area that reflected alarming results.

Highlights
- Future Ni and Pb accumulation was modeled spatially in Türkiye.
- CA-MC was used to model complex dynamics.
- High risk was estimated in the northeast of the area.
- Model results were tested as $R^2 = 0.9412$ for Ni and $R^2 = 0.9882$ for Pb.

Keywords Environmental pollution · Spatial analysis · Sustainable cities · Urban air quality · Tree-rings

Abbreviations

ATRs	Annual Tree Rings
CA	Cellular Automata
HMs	Heavy Metals
MC	Markov Chain
ML	Machine Learning
Ni	Nickel
Pb	Lead
P_{NS}	Nonpoint Source Pollution
RF	Random Forest

✉ Oznur Isinkaralar
obulan@kastamonu.edu.tr

1 Department of Landscape Architecture, Faculty of Engineering and Architecture, Kastamonu University, Kastamonu 37150, Türkiye

2 Department of Environmental Engineering, Faculty of Engineering and Architecture, Kastamonu University, Kastamonu 37150, Türkiye

Introduction

The urgent challenge of pollution caused by heavy metals (HMs), which is a by-product of increasing urbanization (Zheng et al. 2023; Swain 2024), has emerged as a crucial worldwide issue that presents severe threats to both the ecosystem and human health (Ahirvar et al. 2023; Zhang et al. 2023). Monitoring HMs accumulation is a significant issue to prevent human exposure to emerging health risks and reduce the threats posed by new sources (Kadim and Risjani 2022; Liu et al. 2023). Effective management is crucial in addressing the continuous urbanization trends, particularly in developing nations such as Türkiye. However, the EPA identifies nickel (Ni) and lead (Pb) as the 13 Priority Pollutant Metals list (Attaelmanan et al. 2023). Ni levels of more than 1 mg m^{-3} in the air and Pb levels of more than 10 µg dL^{-1} in the blood are considered dangerous (Jain et al. 2020; Subri et al. 2024). Ni is a toxic metal, and Ni compounds, such as Ni sulfide, are suspected to cause cancer (Sulaiman et al. 2023). Waste streams from Ni industries, such as electroplating or textiles, or soil remediation efforts may contain up to 1000 mg L^{-1} of Ni. Environmental regulations require this Ni concentration to be reduced to acceptable levels before discharging the waste (Maus and Werner 2024). Metals threaten the environment and human health by contaminating food chains due to their persistence, toxicity, and bioaccumulation in living organisms (Moldovan et al. 2022). During electroplating, only 30–40% of the metal used is deposited on the articles, while the remaining metal contaminates the rinse waters (Dermentzis 2010). Exposure is vital at this point because of the danger of HMs accumulating without being excreted from the body. Due to its structure, it does not break down and has high toxicity and carcinogenic effects. Pb causes high blood pressure, memory and learning difficulties, kidney failure, amnesia, brain damage, weakness, and nervous system damage; Exposure to Ni -contaminated soils and plants can lead to a range of health issues, including respiratory problems, skin irritation, and even cancer (Nielsen 2009; Moldovan et al. 2022; Balbin et al. 2023; Wang et al. 2024). Therefore, it is necessary to monitor the presence and density of HMs, which can have complex distribution patterns, in spaces used by society and to predict their possible distribution in the future.

As the world converges on this urgent need to tackle various environmental pollutants, traditional assessments, and many technologies are employed to monitor HMs worldwide by utilizing plants as bioindicators. These techniques provide valuable insights into the environmental levels and distribution of HMs, enabling effective monitoring and management programs (Wang et al. 2022). However, air monitoring techniques are especially concerned about the reliability level due to the openness of the air to externalities, and the analysis processes are expensive, affecting all parts of society (Idrees and Zheng 2020). Our research used the ATRs of woody trees to monitor the past. Looking at ATRs, we see the years represented by the trunk. Thus, estimating the environmental conditions the ATRs have been exposed to throughout the tree's life is possible. Based on the measurements determined depending on the years, a future prediction was made for the spatial distributions of Ni and Pb produced. There is a growing number of studies on estimating the spatial distribution of HMs, but these are limited worldwide (Córdoba-Tovar et al. 2023). In this study, measurements in ATRs provided with dendrochronological data were spatialized and modeled with an integrated Cellular Automata (CA)-Markov chain (MC) technique, which is widely preferred in modeling complex processes (Losiri et al. 2016). The CA-MC model is an integrated approach that plays an increasingly crucial role in modeling urban growth, especially in developing countries with different urban characteristics, for forecasting the future based on temporal history. In HMs accumulation, one of the P_{NS}, it is impossible to determine the source, analyze its distribution, and clearly define the dynamics in the cyclical order that can be carried through many channels. However, in this structure, where uncertainties are quite entangled, the temporal-spatial trend sheds light on the results that the complex system produces depending on the initial conditions (Zeng et al. 2023). With the advent of a CA-MC model, several studies have preferred methods for modeling land uses and urban growth (Isinkaralar 2024; Isinkaralar et al. 2024).

In many aspects, obtaining and predicting the closest maps to the real world regarding the spatial distribution of HM concentrations is necessary. First of all, it is indispensable for practical agriculture and environmental management. Notably, urban areas in many cities struggle with serious HMs pollution, mainly due to rapid urbanization, industrial activities, and heavy traffic among contemporary researchers worldwide. Many methods have been applied to future predictions, including the nonparametric spatial prediction method (Liu et al. 2024) and the machine learning (ML) model (Guo et al. 2024; Meng et al. 2024). Bhagat et al. (2021) used algorithms for sedimentary Pb prediction in Bramble and Deception Bays in Australia. Lu et al. (2022) proposed a data-driven concept to predict the flocculation efficiency of HMs ions with the help of an ML model. Xu et al. (2022) created a multi-emission sensor array to detect HMs ions. The prediction approach in these studies focuses on level determination.

This article contributes to the literature on the pollution pattern by using the CA-MC model. It is known that traditional methods that can be used to clean a polluted air, water, or soil environment require a lot of labor and economic capital. In this context, our study has developed a CA-MC model to estimate the spatial pattern where the possible HM risk is high in the future. Thus, it offers strategies for precautions against pollution.

Overview of modeling methodology

The analysis process of this research consists of three stages. Dendrochronology is the stage where samples are collected and prepared following the analysis. In this stage, first of all, it is determined from which locations samples will be considered. The most crucial factor that is effective in site selection is to find the same type of perennial plants. In the study, the pattern of HMs is created by considering the accumulations of the same species in different locations.

For this reason, the plant type is kept constant. After the collected ATRs are cleaned and dried, they are ready for analysis. According to the results of the analysis, pollution levels are determined in the second stage, and spatial distribution maps are produced. Modeling is done in the third stage using the values in the produced maps. As a result of the modeling, pollution estimates are reached in Fig. 1.

Dendrochronology

Ni and Pb, accumulating in living beings, were determined quantitatively by standard dendrochronological methods, considering the tree growth tendency. At this stage, *P. orientalis* L. was selected as the dominant species in the same age group, and the same species and samples were collected from the area. Ni and Pb values represented the most extended ATR chronology since 2018. Trunk samples were taken from each tree at each sampling point, obtaining three samples for validity.

Site selection

Düzce city (40° 50’ 20” N / 31° 9’ 50” E), northwest of Türkiye, was chosen as a case study. Düzce province characterized as an industrial city, is located between the most developed cities of the country: İstanbul and Ankara. It is a transit point in the transportation network connecting many cities to Istanbul. In the last 20 years, the population of the city center has increased 3.25 times. It has a center in a

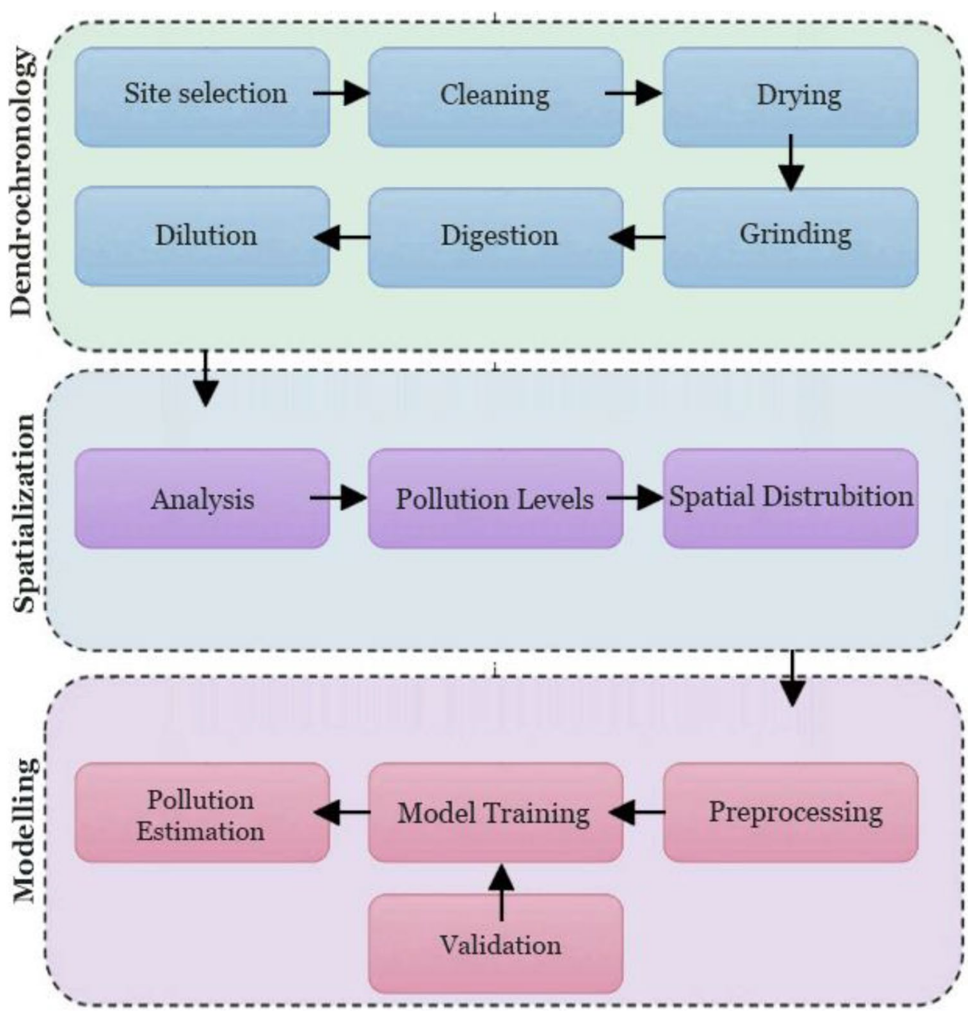

Fig. 1 A methodological framework outlining the steps to process and model data for forecasting Ni and Pb over space and time

Table 1 Coordinates and urban characteristics of the locations

Location	Coordinates	Urban Characteristics			
		Construction	traffic density	Distance to city center	Distance to industry
Loc1	40°50'42.7"N 31°06'50.1"E	L	H	M	L
Loc2	40°50'58.4"N 31°06'58.8"E	M	M	M	H
Loc3	40°51'00.2"N 31°09'54.5"E	NA	H	L	M
Loc4	40°54'14.7"N 31°10'51.8"E	NA	L	H	H
Loc5	40°51'39.4"N 31°12'46.7"E	NA	M	M	H
Loc6	40°48'10.0"N 31°14'15.5"E	NA	H	H	M
Loc7	40°49'55.4"N 31°10'56.0"E	H	H	L	L
Loc8	40°50'23.6"N 31°10'48.8"E	H	H	L	M

L: Low, M: Medium, H: High; NA: Not available

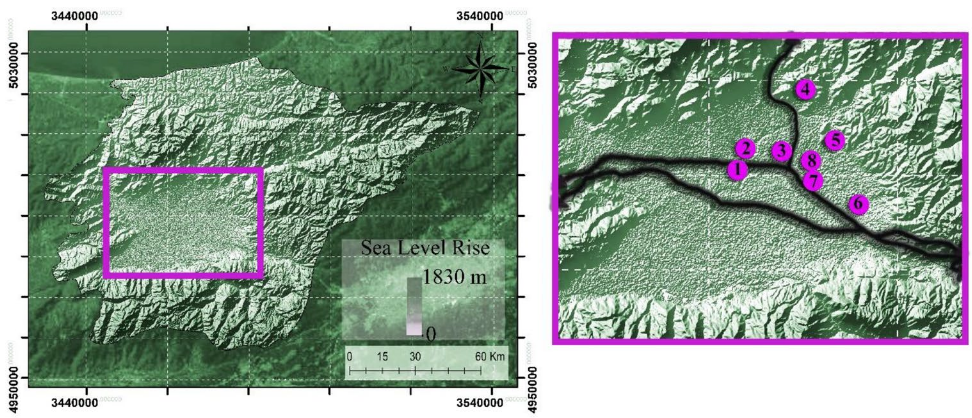

Fig. 2 Map of the modeled study area

depression in a rugged geography, is a coastal city, and has an altitude of 1830 m. In the study, samples were collected from 8 different locations (Loc1 to Loc8) in the city center (Table 1), on the main arteries, from non-urban areas where urban land use differs and can be a reference in measurements in Fig. 2.

Data preparation

Two HMs were selected for this research (Ni and Pb), the most prevalent HMs worldwide and considerably detrimental to human and ecological health (Mngadi et al. 2024). For the Ni and Pb concentration in the tree ring, 0.5 g of each dry sample was utilized with a soft brush with silk bristles and a 5-mm-diameter increment borer at the breast height of different orientations. For each individual, two orthogonal tree cores were collected from the main trunk at a height of 1.2 m above the ground using 5.15 mm stainless steel manual increment borer(CO600, Haglof, Sweden). To visible ATRs (precision of 0.001 mm), polished with sandpaper and allowed to stand open-mouthed at room temperature for two weeks. They were heated again at 45 °C until no moisture for 48 h. Before analysis, the tree-ring fractions were crushed for 3 min (FW177, Pulverizer, China) and sieved through a 0.25 mm nylon mesh for analysis without any contamination. The digestion was carried out with acid mixture, account for 6 mL of 65% HNO_3 (Merck), 2 mL of 30% H_2O_2 (Merck), 2 mL deionized water into the microwave (Ethos One, Milestone GmbH, Germany) for 15 min, as follows: (a) 1 min at 1000 W-75 °C, (b) 4 min at 1000 W-180 °C, (c) 10 min at 1000 W-180 °C, (d) 0 W for 15 min according to 3052 Method USEPA (USEPA 1996). Ni and Pb concentration was measured using atomic emission spectrometry (ICP-OES from SpectroBlue, Spectro, Analytical Instruments GmbH, Germany) with a plasma source device (SpectroBlue, Spectro). For analytical quality control, the obtained sample was analyzed in triplicate, and total metal levels were determined on a dry weight basis. The detection limit for Ni and Pb was 0.81 µg L^{-1} and 2.54 µg L^{-1}.

Dataset

The average values of the measurement results for eight locations in the research area and the standard deviation values calculated based on the measurements made in three replicates are given in Table 2. Our results reveal the accumulated structure of Ni and Pb in metabolism.

According to the analysis, the measurements' concentration levels and standard deviations are presented in Fig. 3. Especially the increasing values for Loc3, where the main arteries are connected, indicate a critical position in the city

Table 2 Measurement results of Ni and Pb accumulation in ATR

Location		Measurements ($\mu g\ kg^{-1}$)											
		Ni						Pb					
		2018	2019	2020	2021	2022	2023	2018	2019	2020	2021	2022	2023
Loc1	x̄	1484.5	1454.2	1403.5	1308.2	1168.1	1001.2	3696.5	3552.3	3586.1	3087.3	2866.4	2379.4
	σ	17.7	12.1	9.7	10.6	21.6	57.6	29.7	37.4	52.5	12.4	59.1	171.2
Loc2	x̄	1450.8	1434.0	1378.2	1305.5	1395.0	1421.2	3646.9	3553.2	3474.2	3438.4	3532.9	3379.9
	σ	3.6	24.6	12.9	21.0	14.4	17.8	27.7	112.2	65.5	34.3	25.0	49.7
Loc3	x̄	1550.7	1491.2	1523.6	1498.8	1450.0	1435.0	4061.5	3791.5	3869.9	3705.4	3638.8	3557.6
	σ	21.7	15.4	5.3	10.6	6.0	7.9	67.3	51.8	84.9	21.3	43.2	2.6
Loc4	x̄	1544.5	1524.5	1498.5	1484.7	1478.3	1432.1	3969.7	3989.8	3800.8	3805.6	3601.3	3536.2
	σ	2.5	33.9	19.9	5.5	12.0	11.6	93.6	44.3	46.9	28.4	47.6	60.4
Loc5	x̄	1424.9	1341.2	1309.4	1230.8	1224.8	1069.5	3812.6	3637.5	3574.4	3302.7	3326.6	2813.6
	σ	13.6	17.3	11.2	11.5	7.4	47.7	44.1	27.4	25.2	61.3	63.7	113.8
Loc6	x̄	1545.5	1504.8	1452.2	1456.1	1400.5	1335.5	4098.8	3999.2	3866.6	3918.9	3758.7	3388.9
	σ	16.4	9.6	17.8	6.3	1.3	9.7	41.1	7.6	76.9	23.4	37.9	62.4
Loc7	x̄	1442.2	1484.9	1417.7	1448.3	1392.5	1376.1	3620.2	3811.2	3535.3	3583.4	3558.9	3435.2
	σ	19.4	20.1	9.8	15.2	11.8	22.5	87.0	36.9	80.1	100.7	38.4	69.6
Loc8	x̄	1502.0	1471.5	1409.6	1432.7	1420.7	1379.5	3954.4	3693.4	3615.1	3562.9	3532.7	3331.1
	σ	20.8	14.6	17.6	23.0	8.4	14.6	72.5	15.5	29.2	35.3	48.0	61.9

x̄: Mean, σ: Standard Deviation

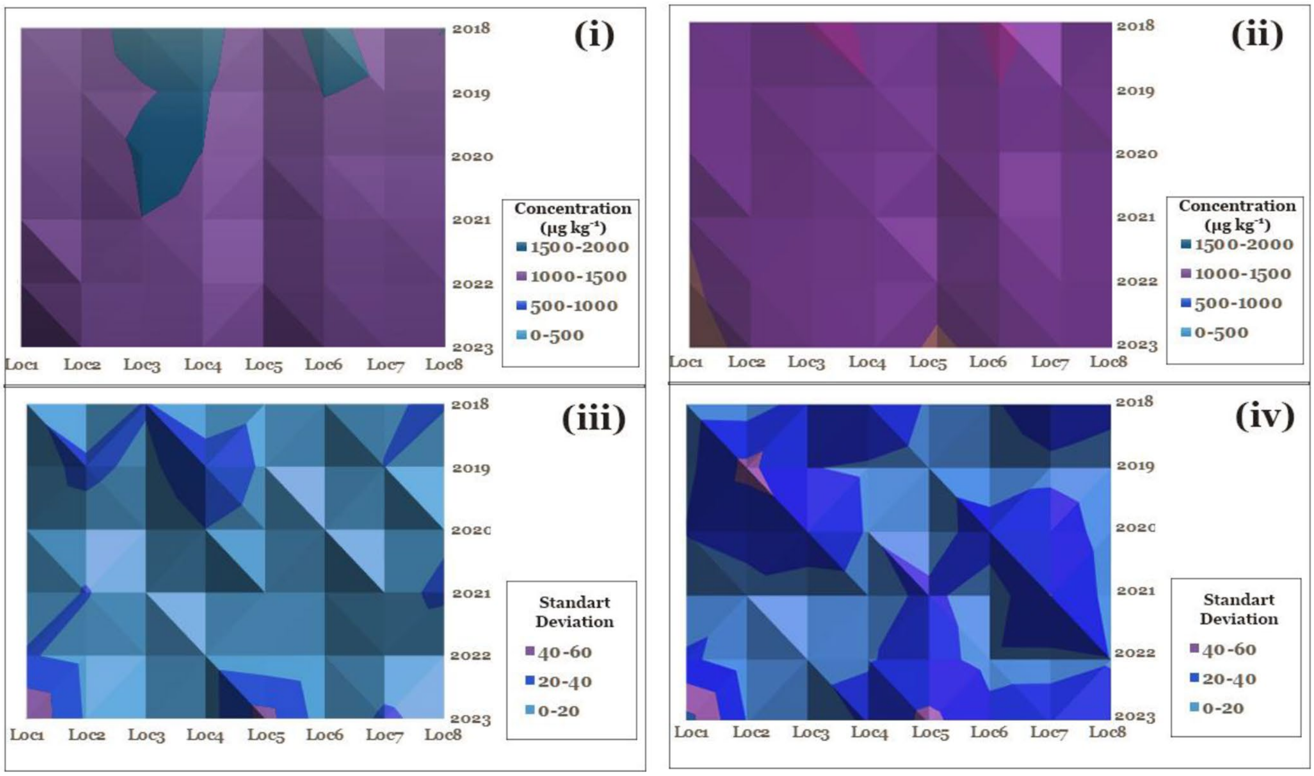

Fig. 3 Concentration levels and standard deviations of the measurements **i**: Ni concentrations; **ii**: Pb concentrations; **iii**: standard deviation of Ni; **iv**: standard deviation of Pb

center in the plain structure. It is observed that the standard deviation values generally do not reach 40–60 µg kg^{-1} values and are between 0 and 10 µg kg^{-1} and 20–40 µg kg^{-1} values throughout the land.

Spatialization: distribution analysis via ArcGIS

The measurement values in the samples taken from eight different points in the city center of Düzce were processed in their locations. Afterward, spatial distribution maps were produced using the spatial analysis tool for data management available in ArcGIS software, version 10.7.1, in this study. The spatial distribution of the concentration of Ni is presented in Fig. 4. The critical increase in Ni distribution in the region located in the center of the field and at the same time at the intersection of urban transportation axes in 2018 is remarkable.

Concentration along the north-south axis and in the eastern part of the area is prominent. In essence, the pollution, especially after 2020, reveals the impact of the increase in urban activities brought about by population accumulation. The spatial distribution of the Pb concentration across the study area is presented in Fig. 5.

Validity of the model

Based on existing research, a model must be validated before it can be used in prediction. In this study, 2023 was selected as a year we know while validating. In the 2023 prediction made using the data in 2018 and 2022, the values were obtained as R^2=0.9412 for Ni and R^2=0.9882 for Pb. There are uncertainties in the predictions, and the models cannot work perfectly. However, for this approach, which aims to produce the closest prediction pattern, the R^2 values are within the acceptable range. Thus, the production of prediction maps can be started, as seen in Fig. 6.

CA-MC modeling

The CA is a dynamic modeling method that can simulate spatial estimates and is one of the oldest known estimation techniques. This approach models the quantity of land category transitions and their spatial distribution over time (Viana et al. 2023). It reveals the changes in neighboring cells by defining the rules in the movements of the past positions of the cells. MCs are effective in estimating the temporal processes using the CA technique. Thus, the advantages of the two methods are combined. In the study, estimates were produced for 2028 using IDRISI 17.0 software. Based

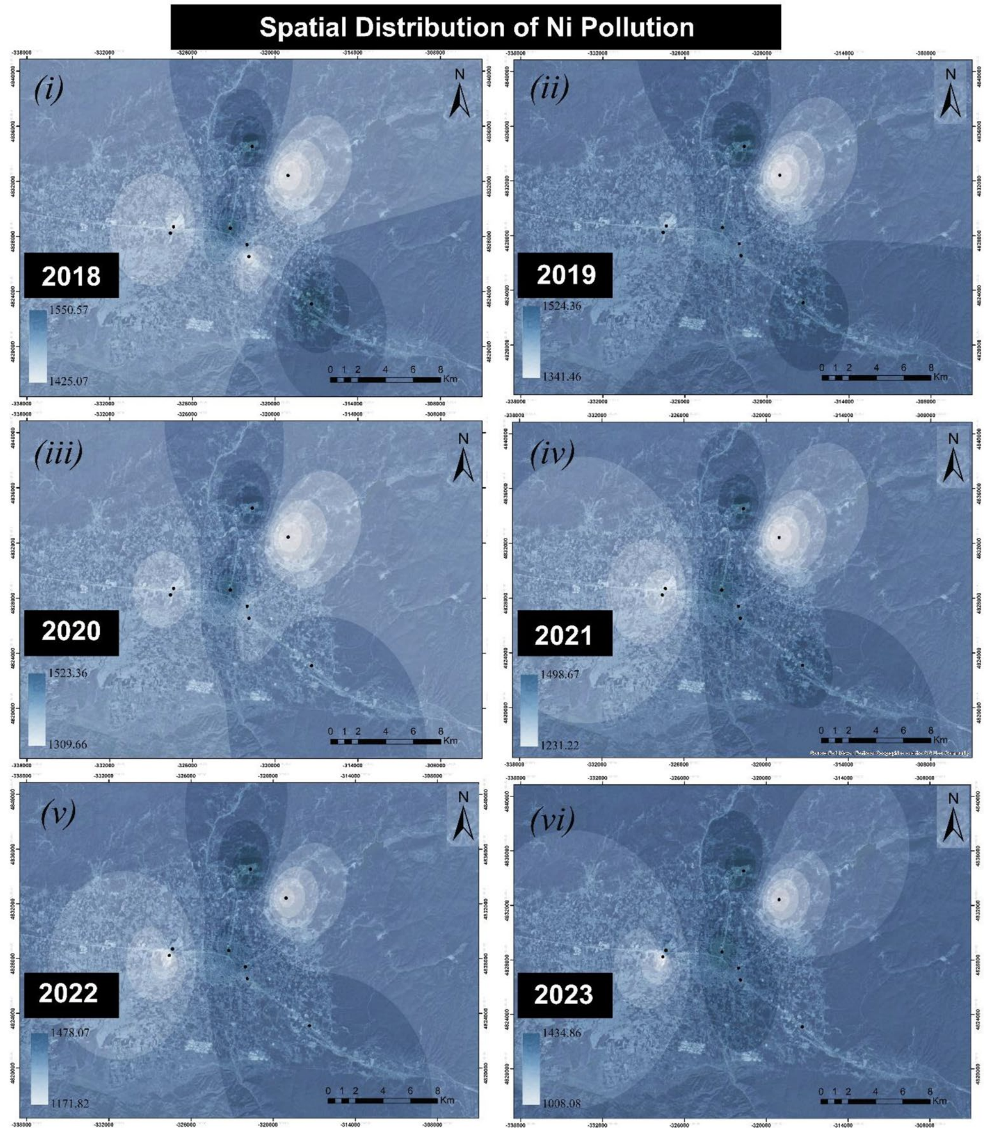

Fig. 4 Spatial distribution and patterns of Ni concentrations (**i** to **vi**:2018 to 2023)

on the texture created by the spatial distributions in the area, the area was divided into 500 × 500 m grids in Fig. 7.

The MC model is a technique that allows us to analyze and reveal the change in land use. The MC process has a principle that can reveal the change prediction based on the probabilities in the transition processes of (t+1) (Moghadam and Helbich 2013):

$$S(t+1) = P_{ij} \times \mathrm{S(t)} \tag{1}$$

Where *S(t)* and *S(t+1)* mean row vectors at time step t and time step *t+1*; P stands for the transition probability matrix for the previous time interval calculated as follows (Adhikari and Southworth 2012):

$$\|Pij\| = \left\| \begin{matrix} P_{11} & P_{12} & P_{1n} \\ P_{21} & P_{22} & P_{2n} \\ P_{n1} & P_{n2} & P_{nn} \end{matrix} \right\| \quad , \quad \left(\mathrm{o} \le P_{ij} < 1 \text{ ve } \sum_{1}^{n} P_{ij} = 1 \right) \tag{2}$$

where *Pij* denotes the probability of transitioning from land-use type *i* to *j*.

The spatial prediction of Ni and Pb distribution for 2028 is presented in Fig. 8, and 9. According to estimates produced using grid-based maps for 2018 and 2023, HM pollution has emerged from the north to the southeast. It is seen that the transportation axes starting from the southwest direction and the industrial activities in the south are effective in the estimate. The effect of traffic and industrial activities, especially on Ni and Pb pollution, will also be reflected in future estimates. The topographic structure of the area is also effective in the formation of densities.

The integrated CA-MC model increases reliability by combining the MC model, which has advantages in temporal processes, with the CA application, which is known for its spatial processability. The reliability of the obtained model was demonstrated by testing. With the method used,

Fig. 5 Spatial distribution and patterns of Pb concentrations (**i** to **vi**:2018 to 2023)

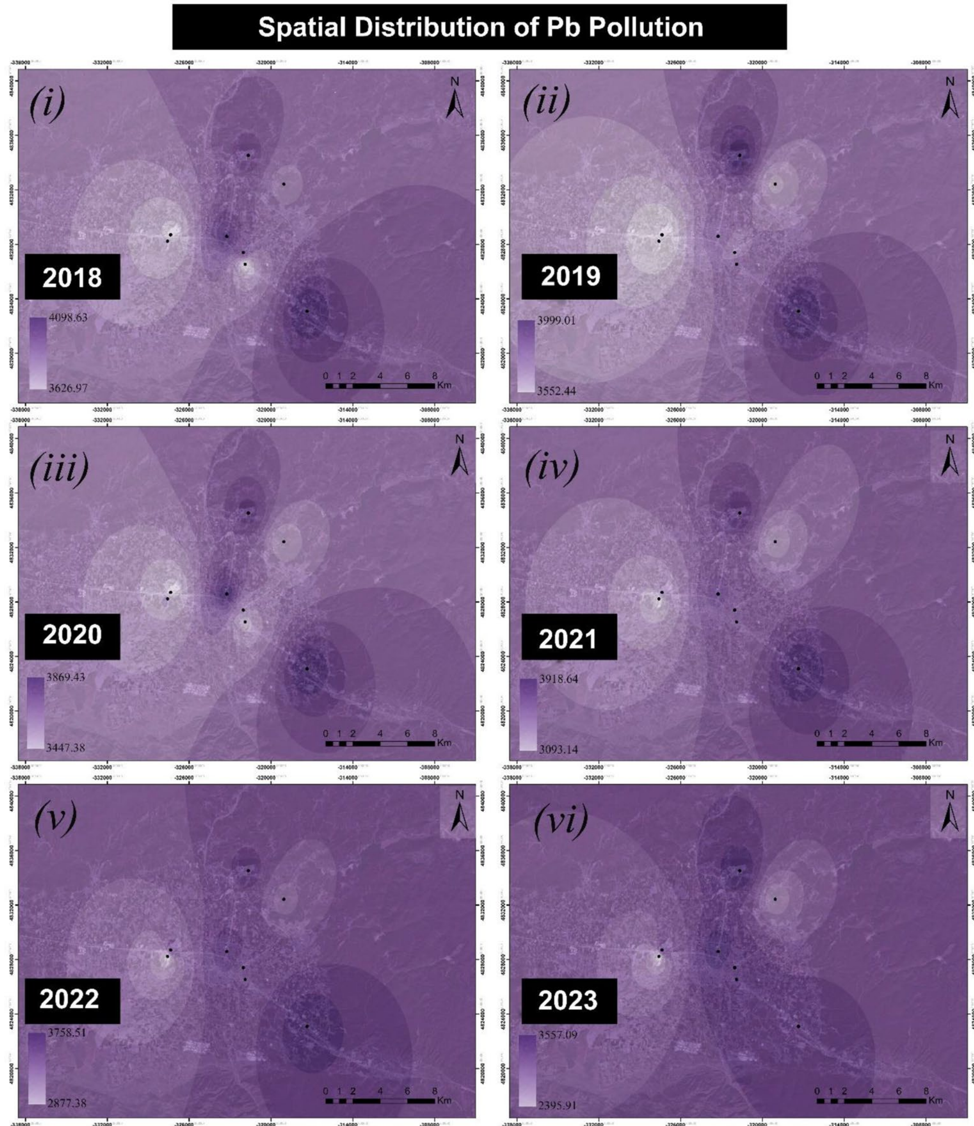

Fig. 6 Evaluating the validity and reliability of the conceptual model through graphical representations (It is a simulation map against the reference map of 2023. Comparison was made for the areal grouping used in grid estimates. **i**: Ni and **ii**: Pb)

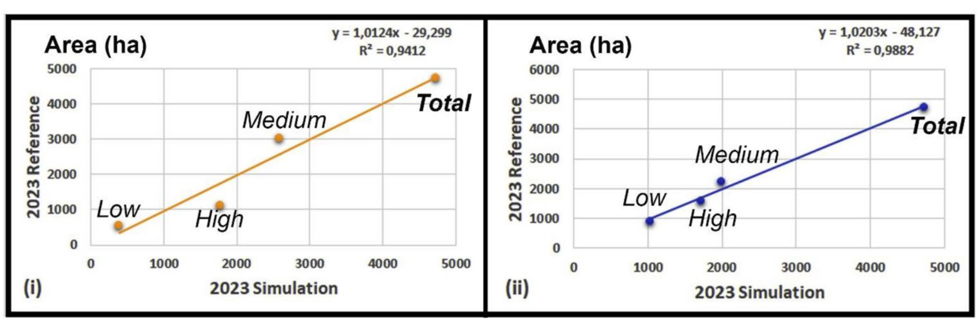

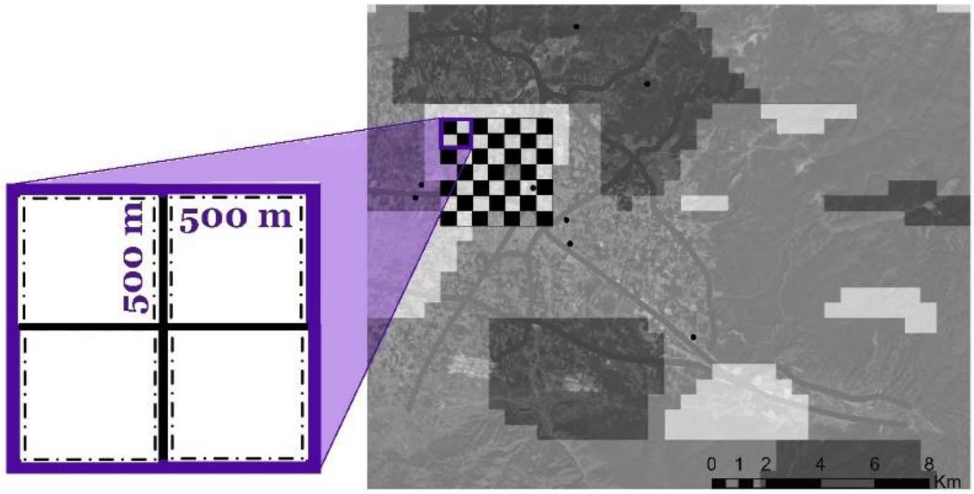

Fig. 7 Summary of the grid technique used in modeling

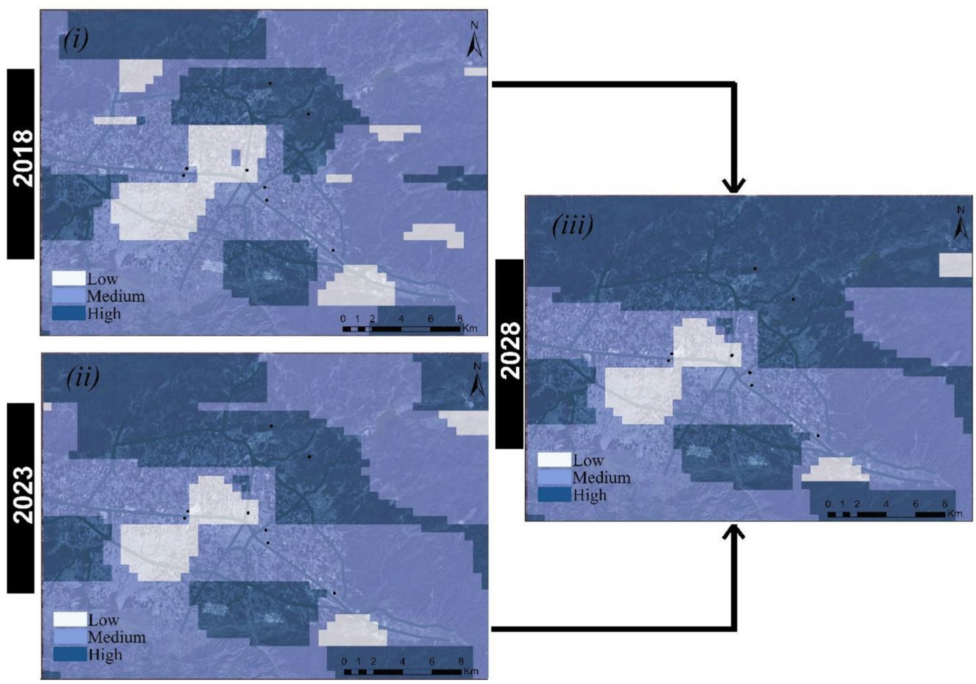

Fig. 8 Spatial prediction of Ni distribution for 2028 (**i**: 2018; **ii**: 2023; **iii**: 2028)

the spatial pattern of how the spatial distribution will be in the future was produced based on grids.

Discussion

Our research is designed to detect spatial patterns and understand natural and anthropogenic sources. Environmental research has long been preoccupied with the spatial patterns of HMs contamination, given the significant consequences these pollutants can have on ecosystems and public health (Wang et al. 2024). The heterogeneous nature of HM distribution in soils has posed a challenge for comprehensive risk assessment and remediation efforts.

One promising approach to understanding and predicting the spatial patterns of HMs contamination is the use of CA-MC modeling, which integrates CA and MC analysis (Mukherjee et al. 2024), coupled with the analysis of ATRs as a proxy for historical HMs deposition (Porru et al. 2024). These studies have highlighted HMs contamination's complex and heterogeneous nature (Goff et al. 2023), often with distinct spatial patterns driven by a combination of natural and anthropogenic factors (Vareda et al. 2019).

From the perspective of ATRs analysis, it has emerged as a valuable tool for reconstructing historical patterns of HM deposition, as the incorporation of metals into the annual growth layers of trees can provide a detailed temporal and spatial record of pollution (Lepp 1975). These studies have highlighted HMs contamination's complex and

Fig. 9 Spatial prediction of Pb distribution for 2028 (**i**: 2018; **ii**: 2023; **iii**: 2028)

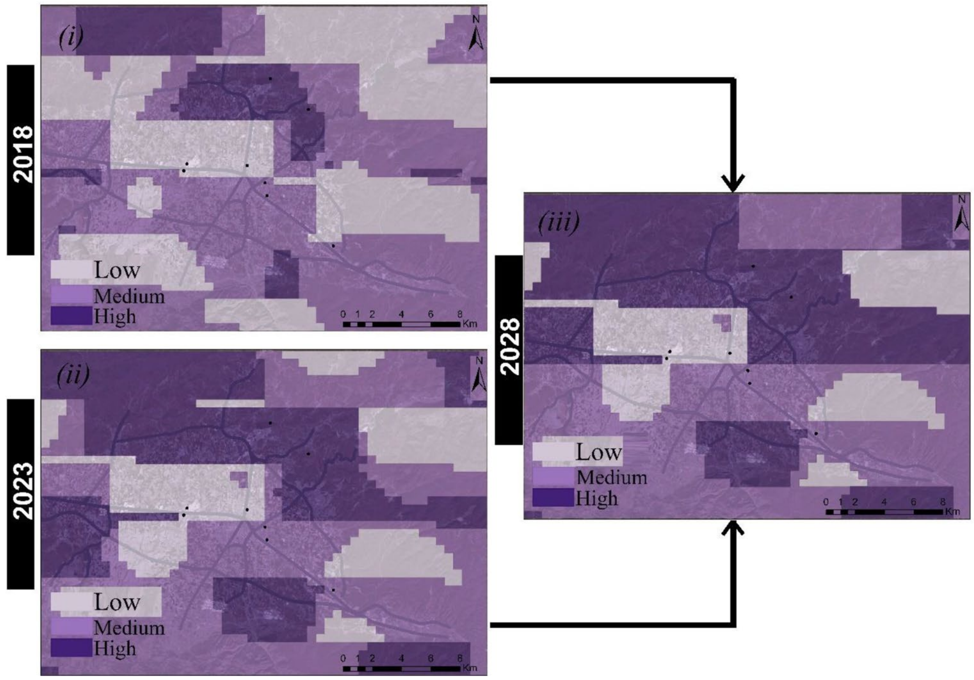

heterogeneous nature, often with distinct spatial patterns driven by natural and anthropogenic sources (Taghizadeh-Mehrjardi et al. 2021). Moreover, the application of multivariate geostatistical analysis has enabled researchers to uncover the underlying relationships between different HM species and their potential sources (Dai et al. 2018). Although Zhang et al. (2020) focus on spatial estimation, they relate the analysis findings to land use and focus on methodological performance. Liu et al. (2022) obtained a risk map for HMs and produced it spatially. However, these studies do not have a perspective on which places the concentrations will increase in the future. They detect high and low-risk areas at points. Jia et al. (2020) used the fuzzy k-means and random forest (RF) methods to determine potential risk areas for HMs pollution. In studies produced with the RF model focusing on spatial estimation (Tan et al. 2020; Wang et al. 2020; Zhang et al. 2021), the aim is to understand the current spatial pattern and temporal dynamics instead of a future estimation. Therefore, the research offers an innovation in this respect.

Previous studies have attempted to show industrial activities and practicalities in HM accumulation. Studies conducted in urban areas of China have revealed the effect of industrial activities on Pb concentrations (Yang et al. 2020). Adhikari et al. (2024) found high Pb concentrations in areas close to urban centers. They emphasize that the spatial variation of Pb varies proportionally with the distance to industrial enterprises (Wu et al. 2020). The main reason is that Pb is an additive in gasoline, paints, and batteries and a by-product of coal combustion. The estimation revealed the tendency of accumulation in the urban center where activities and traffic are intense. For Ni concentrations, the effect of soil parent material was observed. In the last century, with the economic development in the 80s and 90s, the high values of Ni and Pb toxic metal pollution in ATRs have caused fluctuations in the rings of different trees due to small and medium-sized enterprises with severe pollution, rapidly increasing traffic capacities. Chen et al. (2021) sampled *P. massoniana* ATRs for selected ten metals between 1848 and 2016 in Gu Mountain, Fuzhou City. They were categorized into four classes based on a good correlation between environmental pollution and climate conditions: (i) Mn and Sr, (ii) Co, Cd, Pb, (iii) Ni and Cu, (iv) Cr and Fe. Nechita et al. (2021) investigated ATRs of *Q. robur* L. for the deposition of 12 elements, including Ni and Pb, in Romania. Ni and Pb found an increasing trend over the years and indicated similar uptake pathways in trees from industrial activities. The southeast-oriented accumulation and pressure in the main artery in our study were spatially revealed and supported previous findings.

Limitations, future work, and concluding remarks

It is impossible to predict the distribution of HMs perfectly, which can easily change place under the influence of external factors and can occur naturally and humanly. HMs are on the move by participating in many cycles in air, water, and soil and accumulating. Although we cannot reach perfect estimates of the exact value, we can benefit from trees that provide us with the past as a tool to understand urban environments. It is possible to see which exposure locations are high by measuring the accumulation in their metabolism over time. Our work has important implications for policy-makers. However, there are some limitations to this study. First, only ATRs of the *P. orientalis* L. were included in the study to provide valuable information on long-term growth conditions. In future studies, different perennial plants that can be used for monitoring will be selected. The oldest plants in the research area were the same type of plants planted in 2018. Estimates can be produced with a longer term in older settled areas. In addition, grid systems were studied while estimating the data obtained through distribution analyses. In this approach, the value in each grid was accepted as the same to obtain estimates. Finally, the CA-MC method was applied in the future estimate of this study. It is a subject open to research in different frameworks used in spatial estimations and includes geographical features.

Based on the findings of this study help us understand a complex and uncertain subject and offer a new and original methodology. In order for governments to effectively manage public health, it is essential that HM monitoring be carried out systematically. The currently applied detection-based approaches are not sufficient to produce clear strategies. Because in this state, it is impossible to predict the instantaneous exceedance of HMs limits. This research draws attention to the necessity of regular data processing while estimating the spatial pattern of HMs from the starting point.

Authorship contribution Oznur Isinkaralar: Writing– review & editing, Writing– original draft, Visualization, Validation, Software, Resources, Methodology, Investigation, and Formal analysis, Data curation, and Conceptualization. Kaan Isinkaralar: Writing– review & editing, Investigation. Hakan Sevik: Methodology, Investigation, and Data curation.

Data availability All data generated or analyzed during this study are included in this published article.

Declarations

Competing interests The authors declare that they have no known competing financial interests or personal relationships that could have appeared to influence the work reported in this paper.

References

Adhikari K, Mancini M, Libohova Z, Blackstock J, Winzeler E, Smith DR, Owens PR, Silva SHG, Curi N (2024) Heavy metals concentration in soils across the conterminous USA: spatial prediction, model uncertainty, and influencing factors. Sci Total Environ 919:170972. https://doi.org/10.1016/j.scitotenv.2024.170972

Adhikari S, Southworth J (2012) Simulating forest cover changes of Bannerghatta National Park based on a CA-Markov model: a remote sensing approach. Remote Sens 4(10):3215–3243. https://doi.org/10.3390/rs4103215

Ahirvar BP, Das P, Srivastava V, Kumar M (2023) Perspectives of heavy metal pollution indices for soil, sediment, and water pollution evaluation: an insight. Total Environ Res Themes 6:100039. https://doi.org/10.1016/j.totert.2023.100039

Attaelmanan AG, Aslam H, Ali T, Dronjak L (2023) Mapping of heavy metal contamination associated with microplastics marine debris-A case study: Dubai, UAE. Sci Total Environ 891:164370. https://doi.org/10.1016/j.scitotenv.2023.164370

Balbin A, Capilitan J, Taboada E, Tabañag ID (2023) Characteristics of Nickel Laterite Mine Waste in Caraga Region, Philippines and its potential utilization. Nat Environ Pollution Technol 22(3). https://doi.org/10.46488/nept.2023.v22i03.014

Bhagat SK, Tiyasha T, Awadh SM, Tung TM, Jawad AH, Yaseen ZM (2021) Prediction of sediment heavy metal at the Australian bays using newly developed hybrid artificial intelligence models. Environ Pollut 268:115663. https://doi.org/10.1016/j.envpol.2020.115663

Chen S, Yao Q, Chen X, Liu J, Chen D, Ou T, Liu J, Dong Z, Zheng Z, Fang K (2021) Tree-ring recorded variations of 10 heavy metal elements over the past 168 years in southeastern China. Elem Sci Anth 9(1):00075. https://doi.org/10.1525/elementa.2020.20.00075

Córdoba-Tovar L, Marrugo-Negrete J, Barón PAR, Díez S (2023) Ecological and human health risk from exposure to contaminated sediments in a tropical river impacted by gold mining in Colombia. Environ Res 236:116759. https://doi.org/10.1016/j.envres.2023.116759

Dai L, Wang L, Li L, Liang T, Zhang Y, Ma C, Xing B (2018) Multivariate geostatistical analysis and source identification of heavy metals in the sediment of Poyang Lake in China. Sci Total Environ 621:1433–1444. https://doi.org/10.1016/j.scitotenv.2017.10.085

Dermentzis K (2010) Removal of nickel from electroplating rinse waters using electrostatic shielding electrodialysis/electrodeionization. J Hazard Mater 173(1–3):647–652. https://doi.org/10.1016/j.jhazmat.2009.08.133

Goff JL, Chen Y, Thorgersen MP, Hoang LT, Poole FL, Szink EG, Siuzdak G, Petzold CJ, Adams MW (2023) Mixed heavy metal stress induces global iron starvation response. ISME J 17(3):382–392. https://doi.org/10.1038/s41396-022-01351-3

Guo L, Xu X, Niu C, Wang Q, Park J, Zhou L, Lei H, Wang X, Yuan X (2024) Machine learning-based prediction and experimental validation of heavy metal adsorption capacity of bentonite. Sci Total Environ 926:171986. https://doi.org/10.1016/j.scitotenv.2024.171986

Idrees Z, Zheng L (2020) Low cost air pollution monitoring systems: a review of protocols and enabling technologies. J Industrial Inform Integr 17:100123. https://doi.org/10.1016/j.jii.2019.100123

Isinkaralar O (2024) A Methodological Benchmark in determining the Urban Growth: Spatiotemporal projections for Eskişehir, Türkiye. Appl Spat Anal Policy 17(4):1485–1495. https://doi.org/10.1007/s12061-024-09592-9

Isinkaralar O, Isinkaralar K, Yilmaz D, Öztürk S (2024) Multi-dimensional analysis of land use/land cover and urbanization on seasonal variation of land surface temperature in İzmir, Türkiye. Landscape Ecol Eng, 1–18.

Jain D, Kour R, Bhojiya AA, Meena RH, Singh A, Mohanty SR, Rajpurohit D, Ameta KD (2020) Zinc tolerant plant growth promoting bacteria alleviates phytotoxic effects of zinc on maize through zinc immobilization. Sci Rep 10(1):13865. https://doi.org/10.1038/s41598-020-70846-w

Jia X, Fu T, Hu B, Shi Z, Zhou L, Zhu Y (2020) Identification of the potential risk areas for soil heavy metal pollution based on the source-sink theory. J Hazard Mater 393:122424. https://doi.org/10.1016/j.jhazmat.2020.122424

Kadim MK, Risjani Y (2022) Biomarker for monitoring heavy metal pollution in aquatic environment: an overview toward molecular perspectives. Emerg Contaminants 8:195–205. https://doi.org/10.1016/j.emcon.2022.02.003

Lepp NW (1975) The potential of tree-ring analysis for monitoring heavy metal pollution patterns. Environ Pollution (1970) 9(1):49–61. https://doi.org/10.1016/0013-9327(75)90055-5

Liu Z, Fei Y, Shi H, Mo L, Qi J (2022) Prediction of high-risk areas of soil heavy metal pollution with multiple factors on a large scale in industrial agglomeration areas. Sci Total Environ 808:151874. https://doi.org/10.1016/j.scitotenv.2021.151874

Liu S, Wang L, Liu D, Diao J, Jiang Y (2024) A novel spatial prediction method for soil heavy metal based on unbiased conditional kernel density estimation. Sci Total Environ 952:175843. https://doi.org/10.1016/j.scitotenv.2024.175843

Liu P, Wu Q, Hu W, Tian K, Huang B, Zhao Y (2023) Effects of atmospheric deposition on heavy metals accumulation in agricultural soils: evidence from field monitoring and pb isotope analysis. Environ Pollut 330:121740. https://doi.org/10.1016/j.envpol.2023.121740

Losiri C, Nagai M, Ninsawat S, Shrestha RP (2016) Modeling urban expansion in Bangkok metropolitan region using demographic–economic data through cellular automata-Markov chain and multi-layer perceptron-Markov chain models. Sustainability 8(7):686. https://doi.org/10.3390/su8070686

Lu C, Xu Z, Dong B, Zhang Y, Wang M, Zeng Y, Zhang C (2022) Machine learning for the prediction of heavy metal removal by chitosan-based flocculants. Carbohydr Polym 285:119240. https://doi.org/10.1016/j.carbpol.2022.119240

Maus V, Werner TT (2024) Impacts for half of the world's mining areas are undocumented. Nature 625(7993):26–29. https://doi.org/10.1038/d41586-023-04090-3

Meng L, Sheng A, Cao L, Li M, Zheng G, Li S, Chen J, Wu X, Shen Z, Wang L (2024) Contribution assessment and accumulation prediction of heavy metals in wheat grain in a smelting-affected area using machine learning methods. Sci Total Environ 951:175461. https://doi.org/10.1016/j.scitotenv.2024.175461

Mngadi S, Nomngongo PN, Moja S (2024) Elemental composition and potential health risk of vegetable cultivated in residential area situated close to abandoned gold mine dump: characteristics of soil quality on the vegetables. J Environ Sci Health Part B 59(6):300–314. https://doi.org/10.1080/03601234.2024.2339779

Moghadam HS, Helbich M (2013) Spatiotemporal urbanization processes in the megacity of Mumbai, India: a Markov chains-cellular automata urban growth model. Appl Geogr 40:140–149. https://doi.org/10.1016/j.apgeog.2013.01.009

Moldovan A, Török AI, Kovacs E, Cadar O, Mirea IC, Micle V (2022) Metal contents and pollution indices assessment of surface water, soil, and sediment from the Arieș River Basin Mining Area. Romania Sustain 14(13):8024. https://doi.org/10.3390/su14138024

Mukherjee A, Coomar P, Sarkar S, Johannesson KH, Fryar AE, Schreiber ME et al (2024) Arsenic and other geogenic contaminants in global groundwater. Nat Reviews Earth Environ 5(4):312–328. https://doi.org/10.1038/s43017-024-00519-z

Nechita C, Iordache AM, Lemr K, Levanič T, Pluhacek T (2021) Evidence of declining trees resilience under long term heavy metal stress combined with climate change heating. J Clean Prod 317:128428. https://doi.org/10.1016/j.jclepro.2021.128428

Nielsen E (2009) Evaluation of health hazards by exposure to nickel in drinking water. Toxicol Lett. 189(Special Issue) https://doi.org/10.1016/j.toxlet.2009.06.474. S247-S247

Porru S, Esplugues A, Llop S, Delgado-Saborit JM (2024) The effects of heavy metal exposure on brain and gut microbiota: a systematic review of animal studies. Environ Pollut 123732. https://doi.org/10.1016/j.envpol.2024.123732

Subri MSM, Arifin K, Sohaimin MFAM, Abas A (2024) The Parameter of the Sick Building Syndrome: A Systematic Literature Review. Heliyon. https://doi.org/10.1016/j.heliyon.2024.e32431

Sulaiman FR, Mohamed N, Aris AZ (2023) Occurrence, origin, and risk assessment of metals in drinking water from a tropical suburban area (Jengka, Malaysia). Appl Water Sci 13(3):69. https://doi.org/10.1007/s13201-023-01878-6

Swain CK (2024) Environmental pollution indices: a review on concentration of heavy metals in air, water, and soil near industrialization and urbanisation. Discover Environ 2(1):5. https://doi.org/10.1007/s44274-024-00030-8

Taghizadeh-Mehrjardi R, Fathizad H, Ali Hakimzadeh Ardakani M, Sodaiezadeh H, Kerry R, Heung B, Scholten T (2021) Spatio-temporal analysis of heavy metals in arid soils at the catchment scale using digital soil assessment and a random forest model. Remote Sens 13(9):1698. https://doi.org/10.3390/rs13091698

Tan K, Wang H, Chen L, Du Q, Du P, Pan C (2020) Estimation of the spatial distribution of heavy metal in agricultural soils using airborne hyperspectral imaging and random forest. J Hazard Mater 382:120987. https://doi.org/10.1016/j.jhazmat.2019.120987

USEPA (1996) United States Environmental Protection Agency SW-846 test method 3052: Microwave Assisted Acid Digestion of Siliceous and Organically Based Matrices. https://www.epa.gov/hw-sw846/sw-846-test-method-3052-microwave-assisted-acid-digestion-siliceous-and-organically-based. Accessed 11 December 2021

Vareda JP, Valente AJ, Durães L (2019) Assessment of heavy metal pollution from anth ropogenic activities and remediation strategies: A review. J environ manag 246:101–118. https://doi.org/10.1016/j.jenvman.2019.05.126

Viana CM, Pontius RG Jr, Rocha J (2023) Four fundamental questions to evaluate land change models with an illustration of a cellular automata–markov model. Annals Am Association Geographers 113(10):2497–2511. https://doi.org/10.1080/24694452.2023.2232435

Wang H, Yilihamu Q, Yuan M, Bai H, Xu H, Wu J (2020) Prediction models of soil heavy metal (loid) s concentration for agricultural land in Dongli: a comparison of regression and random forest. Ecol Ind 119:106801. https://doi.org/10.1016/j.ecolind.2020.106801

Wang Z, Luo P, Zha X, Xu C, Kang S, Zhou M, Nover D, Wang Y (2022) Overview assessment of risk evaluation and treatment technologies for heavy metal pollution of water and soil. J Clean Prod 379:134043. https://doi.org/10.1016/j.jclepro.2022.134043

Wang Z, Liu J, Yao M, He M, Shang W, Dong X (2024) Indoor air quality and sick-building syndrome at a metro station in Tianjin. China Environ Int 187:108673. https://doi.org/10.1016/j.envint.2024.108673

Wu Z, Chen Y, Han Y, Ke T, Liu Y (2020) Identifying the influencing factors controlling the spatial variation of heavy metals in suburban soil using spatial regression models. Sci Total Environ 717:137212. https://doi.org/10.1016/j.scitotenv.2020.137212

Xu Z, Chen J, Liu Y, Wang X, Shi Q (2022) Multi-emission fluorescent sensor array based on carbon dots and lanthanide for detection of heavy metal ions under stepwise prediction strategy. Chem Eng J 441:135690. https://doi.org/10.1016/j.cej.2022.135690

Yang J, Wang J, Qiao P, Zheng Y, Yang J, Chen T, Lei M, Wan X, Zhou X (2020) Identifying factors that influence soil heavy metals by using categorical regression analysis: a case study in Beijing, China. Front Environ Sci Eng 14:1–14. https://doi.org/10.1007/s11783-019-1216-2

Zeng L, Li K, Guo H, Zhou B, Lyu X, Huo Y, Uhde E, Yang J, Zeren Y, Lu H, Yao D, Qian Z (2023) Contributions of indoor household activities to inhalation health risks induced by gaseous air pollutants in Hong Kong home. Aerosol Air Qual Res 23(9):230063. https://doi.org/10.4209/aaqr.230063

Zhang H, Yin S, Chen Y, Shao S, Wu J, Fan M, Chen F, Gao C (2020) Machine learning-based source identification and spatial prediction of heavy metals in soil in a rapid urbanization area, eastern China. J Clean Prod 273:122858. https://doi.org/10.1016/j.jclepro.2020.122858

Zhang H, Yin A, Yang X, Fan M, Shao S, Wu J, Wu P, Zhang M, Gao C (2021) Use of machine-learning and receptor models for prediction and source apportionment of heavy metals in coastal reclaimed soils. Ecol Ind 122:107233. https://doi.org/10.1016/j.ecolind.2020.107233

Zhang J, Liu Z, Tian B, Li J, Luo J, Wang X, Ai S, Wang X (2023) Assessment of soil heavy metal pollution in provinces of China based on different soil types: from normalization to soil quality criteria and ecological risk assessment. J Hazard Mater 441:129891. https://doi.org/10.1016/j.jhazmat.2022.129891

Zheng F, Guo X, Tang M, Zhu D, Wang H, Yang X, Chen B (2023) Variation in pollution status, sources, and risks of soil heavy metals in regions with different levels of urbanization. Sci Total Environ 866:161355. https://doi.org/10.1016/j.scitotenv.2022.161355

Publisher's note Springer Nature remains neutral with regard to jurisdictional claims in published maps and institutional affiliations.

Springer Nature or its licensor (e.g. a society or other partner) holds exclusive rights to this article under a publishing agreement with the author(s) or other rightsholder(s); author self-archiving of the accepted manuscript version of this article is solely governed by the terms of such publishing agreement and applicable law.